

Statics and dynamics of elastic manifolds in media with long-range correlated disorder

Andrei A. Fedorenko, Pierre Le Doussal, and Kay Jörg Wiese

CNRS-Laboratoire de Physique Théorique de l'Ecole Normale Supérieure, 24 rue Lhomond, 75231 Paris, France

(Dated: January 20, 2007)

We study the statics and dynamics of an elastic manifold in a disordered medium with quenched defects correlated as $\sim r^{-\alpha}$ for large separation r . We derive the functional renormalization-group equations to one-loop order, which allow us to describe the universal properties of the system in equilibrium and at the depinning transition. Using a double $\epsilon = 4 - d$ and $\epsilon = 4 - \alpha$ expansion, we compute the fixed points characterizing different universality classes and analyze their regions of stability. The long-range disorder-correlator remains analytic but generates short-range disorder whose correlator exhibits the usual cusp. The critical exponents and universal amplitudes are computed to first order in ϵ and α at the fixed points. At depinning, a velocity-versus-force exponent larger than unity can occur. We discuss possible realizations using extended defects.

I. INTRODUCTION

Elastic objects in random media are the simplest example of a disordered system exhibiting metastability, glassy behavior, and dimensional reduction, which are difficulties present in a broader class of disordered systems [1, 2, 3]. They can be used to model a remarkable set of experimental systems. Domain walls in magnets behave as elastic interfaces and can experience either random bond disorder (RB) as in ferromagnets with nonmagnetic impurities, or random field disorder (RF) as in disordered antiferromagnets in an external magnetic field [4]. The interface between two immiscible liquids in a porous medium exhibits the same behavior and undergoes a depinning transition as the pressure difference is increased [5]. Charge-density waves (CDW) in solids show a similar conduction threshold [6]. Another example of periodic systems are vortex lines in superconductors which can form different glass phases in the presence of weak disorder [7, 8, 9]. In all these systems, the interplay between elastic forces that tend to keep the system ordered, i.e., flat or periodic, and quenched disorder, which promotes deformations of the local structure, forms a complicated energy landscape with numerous metastable states. This results in glassy properties and a nontrivial response of the system to external perturbations. In particular, the interface becomes rough with displacements growing with the distance x as

$$C(x) \sim x^2; \quad (1)$$

where χ is the roughness exponent. Elastic periodic structures in the presence of disorder lose their strict translational order and form quasi-long-range order characterized by a slow growth of displacements,

$$C(x) = A_d \ln^2 x; \quad (2)$$

where the amplitude A_d is universal in the simplest case. At zero temperature, a driving force f exceeding the threshold value f_c is required to set the elastic manifold into steady motion with a velocity v that vanishes as $v \sim (f - f_c)^z$ at the transition point. The correlation length diverges close to the transition $\xi = \xi_c$ as $\xi \sim |f - f_c|^{-1/\nu}$ and the characteristic time as $\tau \sim \xi^z$, where z is the dynamic critical exponent. Note that the roughness exponent and the universal amplitudes

determined at the depinning transition are in general different from the exponent and amplitudes measured in equilibrium.

Two methods were developed to study the statics of an elastic manifold in a disordered medium. One of them is the Gaussian variational approximation (GVA) performed in replica space, which can be applied to both classes of elastic manifolds, i.e., to interfaces [10] without overhangs and to periodic systems [9, 11]. Within this approach, which is believed to be exact in the mean-field limit, i.e., when the manifold lives in a space of infinite dimensions, metastability is described by breaking of replica symmetry, which allows one to compute the static correlation functions and to obtain different thermodynamic properties. Another method that can be applied to dynamics as well as to statics is the functional renormalization group (FRG) [12]. Simple scaling arguments show that large-scale properties of elastic systems are governed by disorder for $d < d_{uc} = 4$ and that perturbation theory in the disorder breaks down on scales larger than the so-called Larkin scale [13]. To overcome this difficulty, one performs a renormalization-group analysis. It was shown that in this case one has to renormalize the whole disorder correlator that becomes a nonanalytic function beyond the Larkin scale [12, 14, 15, 16]. The appearance of a non-analyticity in the form of a cusp at the origin is related to metastability, and nicely accounts for the generation of a threshold force at the depinning transition. It was recently shown that the FRG can unambiguously be extended to higher loop order so that the underlining nonanalytic field theory is probably renormalizable to all orders [17, 18, 19]. Although the two methods, GVA and FRG, are very different, they provide a fairly consistent picture of the statics, and recently a relation between them was found [20]. There is also good agreement with results of numerical simulations, not only for critical exponents [21, 22, 23] but also for the whole renormalized disorder correlator [24]. However, many questions remain open. Although the dynamics in the vicinity of the depinning transition and at zero temperature is well understood, there is no satisfactory theory for finite temperature, and in particular for the thermal rounding of the depinning transition [25]. It is also remarkable that the exponent χ in experiments on depinning is usually larger than 1, while FRG and numerical simulations of elastic systems with weak disorder give values smaller than 1.

Most studies of elastic manifolds in a disordered medium

treat uncorrelated pointlike disorder. Real systems, however, often contain extended defects in the form of linear dislocations, planar grain boundaries, three-dimensional cavities, etc. It is known that such extended defects, or pointlike defects with sufficiently long-range correlations, can change the bulk critical behavior [26, 27, 28, 29, 30, 31, 32]. Flux lines in superconductors are the most prominent example. The pinning of the flux lines by disorder prevents the dissipation of energy and determines the critical current J_c , which is of great importance for applications. It was found that extended defects produced, for instance, by heavy-ion irradiation, can increase J_c by several orders of magnitude [33]. Systems with anisotropic orientation of extended defects can be described by a model in which all defects are strongly correlated in d_d dimensions and randomly distributed over the remaining $d - d_d$ dimensions. The case $d_d = 0$ is associated with uncorrelated pointlike defects, while extended columnar or planar defects are related to the cases $d_d = 1$ and 2, respectively. The bulk-critical behavior in the presence of this type of disorder was studied in Refs. [26, 27, 28, 29] using a perturbative RG analysis in conjunction with a double expansion in $d = 4 - d_d$ and d_d . The pinning of flux lines by columnar disorder was studied in Ref. [34], where it was shown that the system forms a Bose glass phase with flux lines strongly localized on the columnar defects, resulting in a zero dc linear resistivity. It was argued recently that the topologically ordered glass phase (Bragg glass) formed by flux lines can be destroyed in the vicinity of a single planar defect [35]. It has been shown that the small dispersion in orientation of columnar defects forms a new thermodynamic phase called “splayed glass” [36]. In this phase, the entanglement of flux lines enhances significantly the transport of superconductors [37]. Competition between various types of disorder, point and columnar, has also been studied, at equilibrium [38, 39] and in the moving phases [40].

In the case of an isotropic distribution of disorder, power-law correlations are the simplest example with the possibility for a scaling behavior with new fixed points (FPs) and new critical exponents. The bulk-critical behavior of systems in which defects are correlated according to a power law r^{-a} for large separation r was studied in Refs. [30, 31, 32]. The power-law correlation of defects in d -dimensional space with exponent $a = d - d_d$ can be ascribed to randomly distributed extended defects of internal dimension d_d with random orientation. For example, $a = d$ corresponds to uncorrelated pointlike defects, $a = d - 1$ ($a = d - 2$) describes infinite lines (planes) of defects with random orientation. In general, one would probably not expect a pure power-law decay of correlations. However, if the correlations of defects arise from different sources with a broad distribution of characteristic length scales, one can expect that the resulting correlations will over several decades be approximated by an effective power law [30]. If the correlation function of disorder can be expressed as a finite sum of power-law contributions $\sum_i c_i r^{-a_i}$, one can expect that the scaling behavior is dominated by the term with the smallest a_i [30]. Power-law correlations with a noninteger value $a = d - d_f$ can be found in systems containing defects with fractal dimension d_f [41]. For example, the behavior of ^4He in aerogels is argued to be described by an XY

model with LR correlated defects [42]. This is closely related to the behavior of nematic liquid crystals enclosed in a single pore of aerosil gel, which was recently studied in Ref. [43], using the approximation in which the pore hull is considered a disconnected fractal. Finally, studies of the Kardar-Parisi-Zhang (KPZ) equation with power-law correlations in time [44] bear connections to the case $d = 1$ considered here. However, the perturbative method used there cannot address directly the zero-temperature (strong KPZ coupling) phase, contrary to our present study.

In the present paper, we study the statics and dynamics of elastic manifolds in the presence of (power-law) LR correlated disorder using the FRG approach to one-loop order. The paper is organized as follows. Section II introduces the model. Possible physical realizations are considered in Sec. III. Section IV describes the dynamical formalism and perturbation theory. In Sec. V, we renormalize the theory and derive the FRG equations to one-loop order. In Sec. VI, we study random bond, in Sec. VII, random field, and in Sec. VIII, periodic disorder. In Sec. IX we discuss fully isotropic extended defects. In the final section, we summarize the obtained results and our conclusions.

II. THE MODEL

We consider a d -dimensional elastic manifold embedded in a D -dimensional space with quenched disorder. The configuration of the manifold is described by an N -component displacement field denoted below $u(\mathbf{x})$, or equivalently $u_{\mathbf{x}}$, where \mathbf{x} denotes the d -dimensional internal coordinate of the manifold. For example, a domain wall corresponds to $d = D - 1$ and $N = 1$, a CDW to $d = D$ and $N = 1$, and a flux lattice to $d = D$ and $N = 2$. In what follows, we focus for simplicity on the case $N = 1$ and elastic objects with short-range elasticity. Extensions to $N > 1$ and LR elasticity are straightforward for the statics. The energy of the manifold in the presence of disorder is defined by the Hamiltonian

$$H = \int d^d \mathbf{x} \left[\frac{c}{2} [\nabla u(\mathbf{x})]^2 + V(\mathbf{x}; u(\mathbf{x})) \right]; \quad (3)$$

where c is the elasticity and V is a random potential. In this paper, we study the model where the second cumulant of the random potential has the form

$$\overline{V(\mathbf{x}; u) V(\mathbf{x}^0; u^0)} = R_1 (u - u^0)^d (\mathbf{x} - \mathbf{x}^0) + R_2 (u - u^0) g(\mathbf{x} - \mathbf{x}^0); \quad (4)$$

The first part corresponds to pointlike disorder with short-range (SR) correlations in internal space. The second part corresponds to long-range (LR) disorder in internal space and the function $g(\mathbf{x}) \sim x^{-a}$ at large x with $a > 0$. For convenience, we normalize it so that its Fourier transform is $g(q) = \int d^d \mathbf{x} e^{i\mathbf{q}\cdot\mathbf{x}} g(\mathbf{x}) = \frac{1}{(2\pi)^d}$ at small q with unit amplitude. *A priori* we are interested in the case $a < d$, where the correlations decay sufficiently slowly in internal space. We denote everywhere below $\frac{d^d q}{(2\pi)^d} = \frac{d^d q}{(2\pi)^d}$ and $\frac{d^d \mathbf{x}}{(2\pi)^d} = \frac{d^d \mathbf{x}}{(2\pi)^d}$. The short-scale uv cutoff is implied at q and the size of the system is L .

One could start with model (4), setting $R_1 = 0$; however, as we show below, a nonzero R_1 is generated under coarse graining. Note that the functions $R_1(u)$ can themselves *a priori* be SR, LR, or periodic in the direction of the displacement field u . For SR disorder in internal space only, i.e., $R_2 = 0$, these cases are usually referred to as random bond (RB), random field [$R_1(u) \sim |u|$ at large u] (RF), and random periodic (RP) universality classes. Below we discuss how these classes extend to the case of LR internal disorder (R_2 nonzero).

The model (3) and (4) could easily be studied using presently available numerical algorithms for directed manifolds, in its statics (e.g., exact ground-state determinations) and its dynamics (e.g., critical configuration at depinning), by directly implementing a random potential correlated as described by Eq. (4). It is also interesting to examine which type of correlations in a random medium can naturally lead to Eq. (4) and how such disorder could be realized from, e.g., distributions of extended defects, since some of them may be experimentally feasible.

III. REALIZATIONS AND UNIVERSALITY CLASSES

A. Defect potential

Let us first recall how long-range correlations can arise in the potential created by defects. To this purpose, call $v(r)$ the defect potential, in the simplest case taken to be proportional to defect density. Consider for simplicity a large number of weak defect lines with a uniform and isotropic distribution in a space of dimension D . These create an almost Gaussian random potential $v(r)$ with

$$\overline{v(r)v(r')} = \frac{v_{LR}^2}{r^D} \quad \text{for } r \gg 1 \quad (5)$$

and $a = D - 1$. To derive this, consider defects of finite radius a_d . The probability that point r^0 is contained in the defect going through r is $(a_d/r)^{D-1}$, i.e., inversely proportional to the sphere of radius $r - r^0$. This is easily generalized to isotropic distributions of extended defects of internal dimension a_d , with $a = D - a_d$. Note that by extended defects we mean defects that are perfectly correlated along their internal dimension. Generalizations where defects are themselves (anisotropic) fractals can also be considered.

An important case is a uniform distribution of extended defects in D -dimensional space, but isotropic only within a linear subspace of dimension D^0 . For instance, one can irradiate a material in the bulk while simultaneously rotating it along an axis. This produces a distribution of linear defects ($a_d = 1$), isotropic within the plane ($D^0 = 2$), and normal to the axis (see Fig. 1). More generally, this yields a defect potential with second cumulant,

$$\overline{v(r;z)v(r';z)} = g(r - r')f(z - z'); \quad (6)$$

$$g(r) \sim r^{-a};$$

while $f(z)$ is short-ranged (here $r \in \mathbb{R}^{D^0}$, $z \in \mathbb{R}^{D-D^0}$, $a = D^0 - a_d$).

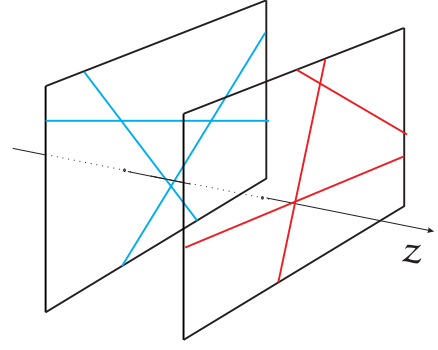


FIG. 1: (Color online) Linear defects randomly and isotropically distributed on parallel planes with random distances between them. This geometry mimics distribution (6).

Although we mostly discuss extended defects, other sources of long-range correlations are possible, such as defects where each single one creates a long-ranged disorder potential, or a substrate matrix itself quenched at a critical point.

B. Coupling to the manifold

We now examine how the long-range correlated defect potential couples to the elastic manifold and what type of LR model results. A general formulation of this coupling (see, e.g., [3]) has the form

$$V(x;u) = \int_{\mathbb{R}^D} d^D z v(x;z) \phi(x;z;u); \quad (7)$$

where the defect potential lives in the D -dimensional space parametrized by $(x;u)$ and $x \in \mathbb{R}^D$ is the internal coordinate of the manifold. $\phi(x;z;u)$ is the manifold density. Each type of coupling to the disorder corresponds to a different function $\phi(x;z;u)$, and we now indicate the main cases.

1. Elastic interfaces in random bond disorder

Let us first discuss elastic interfaces in the so-called random bond (RB) case, where the coupling between disorder and interface occurs only in the vicinity of the interface as, e.g., for domain walls in magnets with random bond disorder. This corresponds to the choice

$$\phi(x;z;u) = \delta(z - u); \quad (8)$$

hence the additional variable z introduced in Eq. (7) is identical to u , the displacement field (with in general $D - D^0 = N$). In that case,

$$V_{RB}(x;u) = v(x;u); \quad (9)$$

Consider now a uniform distribution of defects in the D -dimensional plane but *isotropically distributed within the (averaged direction) of the internal space of the manifold*. This

is given by Eq. (6) above with $D^0 = d$,

$$\overline{V_{RB}(\mathbf{x};u)V_{RB}(0;0)} = g(\mathbf{x})R_2(u); \quad (10)$$

which is model (4) with a SR function $R_2(u)$ and, in full generality, $a = d - 1$. The physical realization in terms of extended defects is thus an interface ($d = 2$) in $D = 3$ with line defects all orthogonal to the u directions, isotropically distributed within the (average) plane of the interface, and $a = 1$. This is illustrated in Fig. 1.

Another physical realization consists of extended defects with finite random lengths such that the distribution of lengths has a power-law tail for large lengths. For instance, needles of variable lengths aligned along one direction could act on a directed polymer $d = 1$ as power-law correlated disorder in internal space.

An interesting, though qualitatively different, case occurs when the extended defects are distributed isotropically in the whole $(\mathbf{x};u)$ space. This will be discussed in Sec. IX. Finally, note that we consider weak Gaussian disorder. It is possible that at strong disorder another phase exists where the line or manifold gets localized along the strongest extended defect.

2. Elastic interfaces in random field disorder

Random field (RF) disorder is described by the function

$$(\mathbf{x};z;u) = (u - z); \quad (11)$$

where (z) is the Heaviside step function. This means that the change in energy when the interface moves between two configurations is proportional to the sum of all defect potentials in the volume (in \mathbb{R}^D) spanned by this change. The discussion of the geometry of defects needed to produce LR disorder in internal space is identical to the last section. Substitution of Eq. (11) into Eq. (7) yields the RF disorder correlator, which can be approximated by Eq. (4) with $R_1(u) = u$ for large u .

3. Periodic systems

As an example of periodic systems, we consider incommensurate single- Q CDWs. In that case $D = d$, hence the function $(\mathbf{x};z;u) = (\mathbf{x};u)$ in Eq. (7). The electron density of CDWs neglecting effects caused by an applied strain has the form [3, 6]

$$(\mathbf{x};) = \rho_0 + \rho_1 \cos[2k_F [\mathbf{x}_\perp - u(\mathbf{x})]g]; \quad (12)$$

where the displacement $u(\mathbf{x})$ of the maximum of the density is related to the standard phase field via $(\mathbf{x}) = 2k_F u(\mathbf{x})$, where k_F is the Fermi wave vector. The d -dimensional space is split into $\mathbf{x} = (\mathbf{x}_k; \mathbf{x}_\perp)$, with \mathbf{x}_\perp denoting the modulation direction of the CDW and k_F the Fermi wave vector.

We again consider the situation of extended defects all aligned with the direction \mathbf{x}_k and isotropically distributed in

that subspace. The random potential experienced by the CDW is given by

$$V(\mathbf{x};) = h_1(\mathbf{x}) \cos(\mathbf{x}) + h_2(\mathbf{x}) \sin(\mathbf{x}); \quad (13)$$

with Gaussian distributed $h_1(\mathbf{x}) = v(\mathbf{x}) \cos(2k_F \mathbf{x}_\perp)$ and $h_2(\mathbf{x}) = v(\mathbf{x}) \sin(2k_F \mathbf{x}_\perp)$. On large scales $k_F \mathbf{x}_\perp \gg 1$, and their cumulant can be approximated by [from Eq. (6)]

$$\overline{h_1(\mathbf{x})h_1(0)} = \frac{1}{2} v_{SR}^2 \delta(\mathbf{x}) + \frac{1}{2} \frac{v_{LR}^2}{x_k^a} \delta(\mathbf{x}_\perp); \quad (14)$$

where we have omitted all rapidly fluctuating contributions. Equations (13) and (14) give the potential correlator in a form that can be generalized to

$$\overline{V(\mathbf{x};u)V(\mathbf{x}^0;u^0)} = R_1(u - u^0) \delta(\mathbf{x} - \mathbf{x}^0) + R_2(u - u^0) g(\mathbf{x}_k - \mathbf{x}_k^0) \delta(\mathbf{x}_\perp - \mathbf{x}_\perp^0); \quad (15)$$

with $d_\perp = 1$ and bare functions $R_1() = \frac{1}{2} v_1^2 \cos()$, u . Thus periodic systems are described by periodic functions $R_1(u)$. Here d_\perp is the dimension of the transverse subspace. Note that the Hamiltonian $H_{XY} = \int d^d x \left[\frac{1}{2} (\nabla \mathbf{x})^2 + V(\mathbf{x};) \right]$ with $V(\mathbf{x};)$ given by Eq. (13) and a Gaussian distribution of fields $\overline{h_1(\mathbf{x})h_1(\mathbf{x}^0)} = g(\mathbf{x} - \mathbf{x}^0)$ describes the XY model with long-range correlated random fields. Therefore, the latter can be mapped onto periodic manifolds with correlator (15) and $d_\perp = 0$, i.e., to model (4) with periodic functions $R_1(u)$. In the next section, we will show how the FRG picture of model (15) can be obtained from the FRG results for model (4). It is worthwhile to note that in the case of periodic systems, the integration in Fourier space is supposed to be over the first Brillouin zone. Note also that we have neglected the coupling of disorder to the long wavelength part of the density $\rho_0 \int d^d x v(\mathbf{x}) r u(\mathbf{x})$ as it is usually irrelevant near the upper critical dimension. Indeed, in the replicated Hamiltonian (see below) this coupling generates additionally to the SR term $\frac{1}{T} \int d^d x \int_0^T r u_a(\mathbf{x}) r u_b(\mathbf{x})$ the LR term

$$\frac{1}{T} \int d^d x \int_0^T d^d x^0 \int_0^T g(\mathbf{x}_k - \mathbf{x}_k^0) \delta(\mathbf{x}_\perp - \mathbf{x}_\perp^0) r u_a(\mathbf{x}) r u_b(\mathbf{x}^0);$$

For small disorder in the vicinity of the upper critical dimension, both of them renormalize to zero according to

$$d_{\perp 1} = (2 - d - 2)_1 + \dots; \quad (16)$$

$$d_{\perp 2} = (2 - a - d - 2)_2 + \dots; \quad (17)$$

IV. DYNAMICAL FORMALISM

The overdamped dynamics of the elastic manifold in a disordered medium can be described by the equation of motion

$$\partial_t u_{xt} = \eta \nabla^2 u_{xt} + F(\mathbf{x};u_{xt}) + f_{xt}; \quad (18)$$

where η is the friction coefficient. In the presence of an applied force f , the center-of-mass velocity is $v = \frac{1}{L^d} \partial_t u_{xt}$. The pinning force reads $F = \partial_u V(\mathbf{x};u)$,

V. FUNCTIONAL RENORMALIZATION

We now consider the renormalization of model (21). The subtleties arising for the correlator (15) will be discussed briefly at the end. We carry out perturbation theory in the bare disorder correlators $\hat{c}_0(u)$ and then introduce the renormalized correlators $\hat{c}_1(u)$. We will suppress the subscript "0" to avoid an overly complicated notation. According to the standard renormalization program, we compute the effective action to one-loop order. Here we adopt the dimensional regularization of integrals and employ the minimal subtraction scheme to compute the renormalized quantities and absorb the poles in $\epsilon = 4 - d$ and $\epsilon = 4 - a$ into multiplicative Z factors. When derivatives of the \hat{c}_1 at $u = 0$ occur, in the dynamics (i.e., at the depinning transition for dynamical quantities) they are taken at $u = 0^+$ as can be justified exactly for $N = 1$. In the statics, the treatment is more subtle (as discussed in two-loop studies [19]) but is not needed in the present one-loop study.

Let us firstly consider the first-order terms generated by expansion of e^S in disorder. These terms are given by diagrams d and e shown in Fig. 2. We start from

$$\begin{aligned} Z & \int_{t > t^0} \int_{\mathbf{x}} \hat{c}_{1,t}(\mathbf{x}, t) \hat{c}_{1,t^0}(\mathbf{x}, t^0) \hat{c}_{1,t}(\mathbf{x}, t) \\ & + \int_{t > t^0} \int_{\mathbf{x}} \hat{c}_{1,t}(\mathbf{x}, t) \hat{c}_{1,t^0}(\mathbf{x}, t^0) g(\mathbf{x}, \mathbf{x}^0) \hat{c}_{1,t^0}(\mathbf{x}, t^0) : (25) \end{aligned}$$

Expanding $\hat{c}_1(u)$ in a Taylor series and contracting one $\hat{c}_{1,t}$ we obtain the leading corrections to the threshold force, friction and elasticity. The terms giving the threshold force to leading order are

$$\begin{aligned} Z & \int_{t > t^0} \int_{\mathbf{x}} \hat{c}_{1,t}(\mathbf{x}, t) \hat{c}_{1,t^0}(\mathbf{x}, t^0) R_{\mathbf{x}=0,t,t^0} \\ & + \int_{t > t^0} \int_{\mathbf{x}} \hat{c}_{1,t}(\mathbf{x}, t) \hat{c}_{1,t^0}(\mathbf{x}, t^0) g(\mathbf{x}, \mathbf{x}^0) R_{\mathbf{x}=\mathbf{x}^0,t,t^0} : (26) \end{aligned}$$

They are strongly uv diverging ($\sim d/2 + a/2$), and thus are nonuniversal. The terms proportional to $\hat{c}_{1,t^0}(\mathbf{x}, t^0)$ can be rewritten as corrections to friction and elasticity using the expansion

$$\begin{aligned} u_{\mathbf{x},t} - u_{\mathbf{x}^0,t^0} &= (t - t^0) \partial_t u_{\mathbf{x},t} + (\mathbf{x} - \mathbf{x}^0)_i \frac{\partial}{\partial x_i} u_{\mathbf{x},t} \\ &+ (\mathbf{x} - \mathbf{x}^0)_i (\mathbf{x} - \mathbf{x}^0)_j \frac{1}{2} \frac{\partial^2 u_{\mathbf{x},t}}{\partial x_i \partial x_j} + O(t^2; \mathbf{x}^3) : (27) \end{aligned}$$

The first term in Eq. (27) gives the correction to friction,

$$\begin{aligned} &= \int_{\mathbf{h}} \hat{c}_{1,t^0}(\mathbf{x}, t^0) \partial_t R_{\mathbf{x}=0,t,t^0} \int_{\mathbf{x}} \hat{c}_{1,t}(\mathbf{x}, t) \partial_t R_{\mathbf{x},t,t^0} g(\mathbf{x}) \\ &= \hat{c}_{1,t^0}(\mathbf{x}, t^0) I_1 + \hat{c}_{2,t^0}(\mathbf{x}, t^0) I_2 ; (28) \end{aligned}$$

where we have introduced $\hat{c}_i(u) = \hat{c}_i(u) = c^2$. The one-loop integrals I_1 and I_2 diverge logarithmically and for $\epsilon; \neq 0$

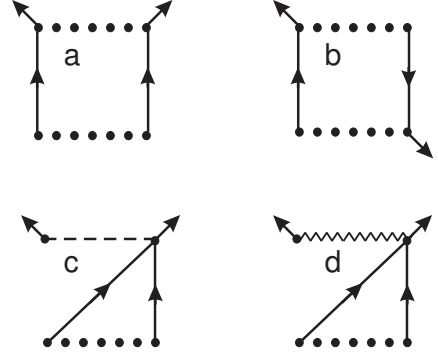


FIG. 3: One-loop diagrams correcting disorder. The dotted line corresponds to either SR disorder vertex (dashed line) or to LR disorder vertex (wavy line). Diagrams of type a, b, and c contribute to SR disorder. Only diagrams of type d correct the LR disorder.

read

$$I_1 = \int_{\mathbf{q}} \frac{1}{(q^2 + m^2)^2} = K_d \frac{m^{-\epsilon}}{\epsilon} + O(1); (29)$$

$$I_2 = \int_{\mathbf{q}} \frac{q^2}{(q^2 + m^2)^2} = K_d \frac{m^{-\epsilon}}{\epsilon} + O(1); (30)$$

where we set $m = m = \frac{P}{c}$ and K_d is the area of a d -dimensional sphere divided by $(2)^d$. To remove the poles in the mobility, we introduce the corresponding Z factor $Z_R = Z^{-1} [I_1]$, which to one-loop order is given by

$$Z^{-1} = 1 - \hat{c}_{1,t^0}(\mathbf{x}, t^0) I_1 - \hat{c}_{2,t^0}(\mathbf{x}, t^0) I_2 : (31)$$

In the absence of LR correlated disorder, the elasticity remains uncorrected to all orders due to the STS, while here the correction reads

$$\begin{aligned} c &= \frac{1}{2d} \int_{\mathbf{q}} \hat{c}_{2,t^0}(\mathbf{x}, t^0) \mathbf{x}^2 R_{\mathbf{x},t,t^0} g(\mathbf{x}) \\ &= \frac{1}{2d} \int_{\mathbf{q}} \hat{c}_{2,t^0}(\mathbf{x}, t^0) g(\mathbf{q}) \mathbf{x}^2 \frac{1}{q^2 + m^2} \\ &= \frac{K_d}{d} \hat{c}_{2,t^0}(\mathbf{x}, t^0) \frac{m^{-\epsilon}}{\epsilon} : (32) \end{aligned}$$

We have not set the second derivative at 0^+ as \hat{c}_2 remains analytic as is discussed below. Furthermore, the correction to elasticity (32) is finite for $\epsilon; \neq 0$, and thus c does not acquire an anomalous dimension. However, we expect corrections at two-loop order. If this is the case, one has to introduce a Z -factor that renormalizes elasticity: $c_R = Z_c^{-1} [I_3] c$ with $Z_c = 1 + O(\frac{\epsilon}{2})$.

In principle, due to the lack of STS, the KPZ term $(\partial_t u_{\mathbf{x},t})^2$ breaking the symmetry $u \rightarrow -u$ can be generated in the equation of motion (18) at the depinning transition. Indeed, diagram e in Fig. 2, when expanding $\hat{c}_1(u)$ to second order in u , using Eq. (27), gives

$$= \frac{1}{2d} \int_{\mathbf{q}} \hat{c}_{2,t^0}(\mathbf{x}, t^0) \mathbf{x}^2 R_{\mathbf{x},t,t^0} g(\mathbf{x}) : (33)$$

Moreover, the term with cubic symmetry ($M = 2$) and terms with higher-order symmetries ($M > 2$) can be generated by diagram e,

$$M = \frac{1}{d(2M)!} \int \frac{d^d x}{(2\pi)^d} R_{x,t} g(x) x_i^{2M} : (34)$$

However, as we will show later, if we start from bare analytic disorder distribution, the LR disorder remains analytic along the FRG flow and the corresponding FP value $\tilde{z}_2(u)$ is also an analytic function. Thus terms (33) and (34) are zero, provided that they are absent in the beginning. Moreover, the terms (34) are irrelevant in the RG sense for $M > 2$ [but not the KPZ term (33); see Ref. [46]]. This proves that our bare model (21) is a minimal model for the description of elastic manifolds in a random media with LR correlated disorder.

The corrections to disorder are given by the diagrams shown in Fig. 3. The corresponding expressions read

$$\begin{aligned} \hat{1} \hat{1}(u) &= \hat{f}_1^0(u)^2 + [\hat{1}(u) \hat{1}(0)] \hat{1}^{\text{oo}}(u) g I_1 \\ &\quad + \hat{f}_2^0(u) \hat{2}^0(u)^2 + [\hat{2}(u) \hat{2}(0)] \hat{2}^{\text{oo}}(u) \\ &\quad + \hat{1}(u) \hat{2}^{\text{oo}}(u) g I_2 + \hat{1}^0(u)^2 + \hat{2}(u) \hat{2}^{\text{oo}}(u) I_3; (35) \\ \hat{1} \hat{2}(u) &= \hat{1}(0) \hat{2}^{\text{oo}}(u) I_1 + \hat{2}(0) \hat{2}^{\text{oo}}(u) I_2; (36) \end{aligned}$$

The one-loop integrals I_1 and I_2 have been defined in Eqs. (29) and (30), whereas I_3 is given by

$$I_3 = \int \frac{d^d q}{(2\pi)^d} \frac{q^{2(a-d)}}{(q^2 + m^2)^2} = \frac{K_4 m^{2-d}}{2} + O(1); (37)$$

Let us define the renormalized dimensionless disorder R_i as

$$m^{-\frac{d}{2}} R_1 = \hat{1}(u) + \hat{1} \hat{1}(u); (38)$$

$$m^{-\frac{d}{2}} R_2 = \hat{2}(u) + \hat{1} \hat{2}(u); (39)$$

The \hat{i} functions are defined as the derivative of $R_i(u)$ with respect to the mass m at fixed bare disorder $\hat{i}(u)$. In order to attain a fixed point, it is necessary to rescale the field u by $m^{-\frac{d}{2}}$ and write the functions for the functions $\tilde{z}_i = R_i(u m^{-\frac{d}{2}})$,

$$\partial_u \tilde{z}_1(u) = \left(-\frac{d}{2} \tilde{z}_1(u) + u \tilde{z}_1^0(u) + \frac{1}{2} \frac{d^2}{du^2} [\tilde{z}_1(u) + \tilde{z}_2(u)]^2 + A \tilde{z}_1^{\text{oo}}(u) \right); (40)$$

$$\partial_u \tilde{z}_2(u) = \left(-\frac{d}{2} \tilde{z}_2(u) + u \tilde{z}_2^0(u) + A \tilde{z}_2^{\text{oo}}(u) \right); (41)$$

where $A = [\tilde{z}_1(0) + \tilde{z}_2(0)]$ and $\partial_u \equiv \frac{d}{du}$.

The scaling behavior of the system is controlled by a stable fixed point $[\tilde{z}_1(u); \tilde{z}_2(u)]$ of flow equations (40) and (41). To determine the critical exponents, let us start from power counting following Ref. [46]. The quadratic part of action (21) is invariant under $x \rightarrow x b$, $t \rightarrow t b^z$, $u \rightarrow u b$, $\hat{u} \rightarrow \hat{u} b^{2-z}$. Under this transformation, the mobility, elasticity, and disorder scale at the Gaussian FP as $c \rightarrow c b$, $\hat{c} \rightarrow \hat{c} b^{z+1}$, $\tilde{z}_1 \rightarrow \tilde{z}_1 b^{d/2+2}$, and $\tilde{z}_2 \rightarrow \tilde{z}_2 b^{d/2+2}$. Thus SR disorder becomes relevant for $d < 4$ and LR disorder is naively relevant for $d > 2$.

Note that in the presence of STS, $\tilde{z}_i = 0$, and we recover the conditions obtained at the end of Sec. III. The actual value of \tilde{z}_i will be fixed by the disorder correlators at the FP. The elasticity exponent ν and the dynamic exponent z read

$$\nu = m \frac{d}{dm} \ln Z_c(\tilde{z}_i)_0; (42)$$

$$z = 2 + m \frac{d}{dm} \ln Z(\tilde{z}_i)_0; (43)$$

where subscript “0” means a derivative at constant bare parameters. To one-loop order this yields

$$\nu = O(m^2; m^{-2}); (44)$$

$$z = 2 - \tilde{z}_1^{\text{oo}}(0) - \tilde{z}_2^{\text{oo}}(0); (45)$$

The scaling relations then read [46]

$$\nu = \frac{1}{2 + \nu}; (46)$$

$$\nu = (z - 2) = \frac{z}{2 + \nu}; (47)$$

At zero velocity, the above calculation can be considered as a dynamical formulation of the equilibrium problem. However, one has to be careful with mapping the dynamic FRG equations to the static equations, because as shown in Ref. [19] the bare relation $\hat{1} = R_1^{\text{oo}}(u)$ breaks down for the SR case at two-loop order. The standard derivation of the FRG equations in the statics is based on the renormalization of the replicated Hamiltonian. We have checked that similar to other systems with only SR disorder, the static FRG equations for systems with LR disorder can be obtained from the dynamic flow equations to one-loop order using the identification $\tilde{z}_i = R_i^{\text{oo}}(u)$. They read

$$\partial_u R_1(u) = \left(-\frac{d}{2} R_1(u) + u R_1^0(u) + \frac{1}{2} [R_1^{\text{oo}}(u) + R_2^{\text{oo}}(u)]^2 + A R_1^{\text{oo}}(u) \right); (48)$$

$$\partial_u R_2(u) = \left(-\frac{d}{2} R_2(u) + u R_2^0(u) + A R_2^{\text{oo}}(u) \right); (49)$$

where $A = [R_1^{\text{oo}}(0) + R_2^{\text{oo}}(0)]$.

In the case of the model with correlator given by Eq. (15), one has to distinguish between the transverse and parallel directions, and therefore introduce corresponding elastic coefficients c_\perp and c_\parallel . In the transverse direction, disorder is only \perp -correlated and as a result the transverse elasticity is not corrected and can be set to 1. The power counting shows that the LR disorder is naively relevant for $d_1 = 4 - d_\perp - a < 0$. The one-loop integrals are logarithmically divergent and for $d_1 \neq 0$ are given by Eqs. (29), (30), and (37) with $d_1 \rightarrow 1$. Thus the above renormalization can be generalized to model (15) if one formally replaces $d_1 \rightarrow 1$.

Let us show how a nonanalyticity of the disorder appears in the problem. We start from the bare analytic correlators with $\tilde{z}_i^{\text{oo}}(0) < 0$. The flow equation for $\tilde{y} = \tilde{z}_1^{\text{oo}}(0) - \tilde{z}_2^{\text{oo}}(0)$ $R_1^{\text{oo}}(0) + R_2^{\text{oo}}(0) > 0$ reads

$$\partial_u \tilde{y} = -\tilde{y} + 3\tilde{y}^2 + \tilde{m}(u); (50)$$

where $\gamma_2(u) = \gamma_2^{\text{FP}}(0)$. As we show below, the function $\gamma_2(u)$ remains analytic along the whole FRG flow and at the fixed point (FP). The solution of Eq. (50) for any function $\gamma_2(u)$ bounded from below blows up at some finite scale u , which can be associated with the inverse Larkin length. This blowup of γ corresponds to the generation of a cusp singularity: $\gamma_1(u)$ becomes nonanalytic at the origin and acquires for $u < u^*$ a nonzero $\gamma_1^0(0^+)$. The precise estimation of the Larkin scale requires the solution of the pair of flow equations for both $\gamma_i(u)$.

Before studying different FPs, let us note an important property that is valid under all conditions: if $\gamma_i(u)$ ($i = 1, 2$) is a solution of Eqs. (40) and (41), then $\gamma_i(u) = x \gamma_i(u)$ is also a solution. Analogously, if $R_i(u)$ is a solution of Eqs. (48) and (49), then $R_i(u) = x R_i(u)$ is also a solution. We can use this property to fix the amplitude of the function in the nonperiodic case, while for the periodic case the solution is unique as the period is fixed.

VI. NONPERIODIC SYSTEMS: RANDOM BOND DISORDER

In this section, we study the scaling behavior of an elastic interface in a disordered environment with LR correlated RB disorder. To this aim, we have to find a stationary solution (FP) of Eqs. (48) and (49) that decays exponentially fast at infinity as expected for RB disorder. The SR RB FP with $R_2(u) = 0$, which describes systems with only SR correlated disorder, was computed numerically in Refs. [12, 17, 18]. The corresponding roughness exponent to one-loop order is given by $\nu_{\text{SR}} = 0.208298 + O(\epsilon^2)$. We now look for a LR RB FP with $R_2(u) \neq 0$. Integrating Eq. (49), we obtain

$$\partial_u R_2(u) = \left(\frac{5}{2} - \frac{1}{2} \right) R_2(u); \quad (51)$$

Therefore, the new LR RB FP, if it exists, has

$$R_2(u) = \frac{1}{5} + O(u^2); \quad (52)$$

The direct inspection of diagrams contributing to the FRG equation for R_2 shows that the higher orders can only be linear in even derivatives of $R_2(u)$. The only term that is linear in $R_2(u)$ comes from the renormalization of the elasticity and can be rewritten as $2 R_2(u)$ to all orders. Therefore, in higher orders we have

$$\partial_u R_2(u) = \left(\frac{5}{2} + 2 \right) R_2(u); \quad (53)$$

and as a consequence, $\int_0^{R_1} du R_2(u)$ is exactly preserved along the FRG resulting in the exact identity

$$R_2(u) = \frac{1}{5} + \frac{2}{5} u; \quad (54)$$

Using our freedom to rescale $R_i(u)$, we introduce $\hat{R}_i(u) = R_i(u)/x$ and fix $\hat{R}_1^0(0) = 1$ and $\hat{R}_2^0(0) = 1$, where x is the parameter to be determined. The stationarity condition of Eqs. (48) and (49) reads

$$\frac{1}{5} \hat{R}_1(u) + \frac{1}{5} u \hat{R}_1^0(u) + \frac{1}{2} [\hat{R}_1^0(u) + \hat{R}_2^0(u)]^2 + (1+x) \hat{R}_1^0(u) = 0; \quad (55)$$

$$\frac{1}{5} \hat{R}_2(u) + \frac{1}{5} u \hat{R}_2^0(u) + (1+x) \hat{R}_2^0(u) = 0; \quad (56)$$

Since Eq. (56) is linear in \hat{R}_2 , it can be solved for fixed x by

$$\hat{R}_2(u) = \frac{5(1+x)}{10} \exp\left(-\frac{u^2}{10(1+x)}\right); \quad (57)$$

From the Taylor expansion of Eq. (55) around $u = 0$, we find

$$\begin{aligned} \hat{R}_1^0(0) &= \frac{5(1+x)}{8}; \\ \hat{R}_1^0(0) &= 0; \end{aligned} \quad (58)$$

where the second condition excludes the possibility of a supercusp (the first line does not diverge since $x = 1$ for $\epsilon = 5$). Thus for fixed \hat{R}_1^0 the simultaneous equations (55) and (56) have a unique solution for any x , but only for a specific x does the solution $\hat{R}_1(u)$ decay exponentially fast to 0 for large u . To determine this value, we employ the shooting method choosing x as our shooting parameter. For fixed x , we integrate numerically Eq. (55) with $\hat{R}_2(u)$ given by Eq. (57) from 0 to some large u_{max} with initial conditions (58). Then the shooting parameter x can be found by solving numerically the algebraic equation $\hat{R}_1(u_{\text{max}}; x) = 0$. Increasing u_{max} , we acquire the desired accuracy for x and $\hat{R}_1(x)$. We were able to find the numerical solution with reasonable accuracy only for $\epsilon = 1.1$. The typical FP functions $\hat{R}_1(u)$ and $\hat{R}_2(u)$ are shown in Fig. 4. The actual values of x obtained by shooting for different ϵ are summarized in Table I.

Let us now check the stability of SR and LR FPs. To that end we linearize the FRG equations about each FP. In the vicinity of a FP, the linearized flow equations have solutions that are pure power laws in u , i.e., scale as u^λ with a discrete spectrum of eigenvalues λ . A stable fixed point has all eigenvalues $\lambda < 0$. Substituting $\hat{R}_i(u) = \hat{R}_i^0(u) + z_i(u)$ into the flow equations and keeping only terms that are linear in $z_i(u)$, we derive the linearized flow equations at the FP $f_{R_1(u)}; R_2(u)g$,

$$\begin{aligned} (1 - \frac{1}{5}) z_1(u) + \frac{1}{5} u z_1^0(u) + [\hat{R}_1^0(u) + \hat{R}_2^0(u)] \\ [\hat{R}_1^0(u) + \hat{R}_2^0(u)] + (1+x) z_1^0(u) \\ + A_0 \hat{R}_1^0(u) = z_1(u); \end{aligned} \quad (59)$$

$$\begin{aligned} (\frac{1}{5} - \frac{1}{5}) z_2(u) + \frac{1}{5} u z_2^0(u) \\ + (1+x) \hat{R}_2^0(u) + A_0 \hat{R}_2^0(u) = z_2(u); \end{aligned} \quad (60)$$

where we have introduced $\lambda = \frac{1}{5}$, $A_0 = [\hat{R}_1^0(0) + \hat{R}_2^0(0)]$ and λ is also measured in units of ϵ . Note that because

TABLE I: Long-range correlated random bond fixed point. Shooting parameter $x = r_1^{(0)}(0)$, the maximal eigenvalue and the universal amplitude for different values of \hat{a} .

\hat{a}	$x(\hat{a})$	λ_1	$B(\hat{a})$
1.1	1.931986		33.89
1.2	1.121722	0.160	31.37
1.3	0.922046	0.262	31.64
1.4	0.825747	0.365	32.41
1.5 ^a	0.766976	0.469	33.34
2.0 ^b	0.639151	1	38.44
3.0 ^c	0.562357	2.120	48.10
1	0.463619	1	

^aRandom lines in a planar interface ($d = 2, a = 1$).

^bRandom lines in a 3d manifold ($d = 3, a = 2$).

^cRandom planes in a 3d manifold ($d = 3, a = 1$).

of the freedom to rescale $r_1(u)$, we always have the eigenmode $z_1^{(0)}$ with marginal eigenvalue $\lambda_0 = 0$. As shown in Ref. [45] for SR RB FP the corresponding eigenfunction is given by $z_1^{(0)} = u r_1^{(0)}(u) - 4 r_1(u); z_2^{(0)} = 0$, while the next eigenvalue $\lambda_1 = 1$ corresponds to $z_1^{(1)} = \frac{5}{3} u r_1^{(0)}(u) + (1 - 4 \frac{5}{3}) r_1(u); z_2^{(1)} = 0$. Here $f r_1; r_2 = 0g$ is the SR RB FP and the Taylor expansion of the function r_1 can be found in Ref. [45]. Thus the SR RB FP is stable in the SR disorder subspace ($r_2 = z_2 = 0$). Let us check its stability with respect to introduction of LR correlated disorder. From Eq. (60) it follows that the maximal eigenvalue $\lambda_{\max} = \hat{a} \frac{5}{3} \frac{5}{3}$ corresponds to the exponential eigenfunction $z_2(u) = \exp(\frac{5}{3} u^2 - 2 r_1^{(0)}(0))$ with $r_1^{(0)}(0) = 0.577$ for SR RB FP. As a consequence, the LR correlated disorder destabilizes the SR RB FP if $\hat{a} > \frac{5}{3} \frac{5}{3} = 1.041$, or equivalently, using Eq. (52), if $\frac{5}{3} < \frac{5}{3}$. This criterion was of course expected.

We now check the stability of the LR RB FP $f r_1(u); r_2(u) \neq 0g$. It also has a marginal eigenvalue $\lambda_0 = 0$ with eigenfunctions given by $z_1^{(0)} = u r_1^{(0)}(u) - 4 r_1(u)$ that can be checked by direct substitution into Eqs. (59) and (60). Equation (60) allows for an analytical solution that reads

$$z_2(u) = \frac{5A_0}{2^{\hat{a}+5}} \frac{u^2}{5(1+x)} \frac{1}{1} \exp \frac{u^2}{10(1+x)} \quad (61)$$

We are free to fix the length of the eigenvectors, for instance, by the condition $z_2^{(0)}(0) = 1$, which gives

$$A_0 = \frac{1}{3^{\hat{a}}} (1+x) [2^{\hat{a}+5}] : \quad (62)$$

Thus to find the eigenvalue λ_1 and the eigenfunction z_1 , we have to solve Eq. (59) with condition $z_1^{(0)}(0) = 1 - A_0$ and require an exponentially fast decay of the solution at large u . The only case for which we succeeded to construct the solution analytically is $\hat{a} = 2$, which is depicted in Fig. 5. It has

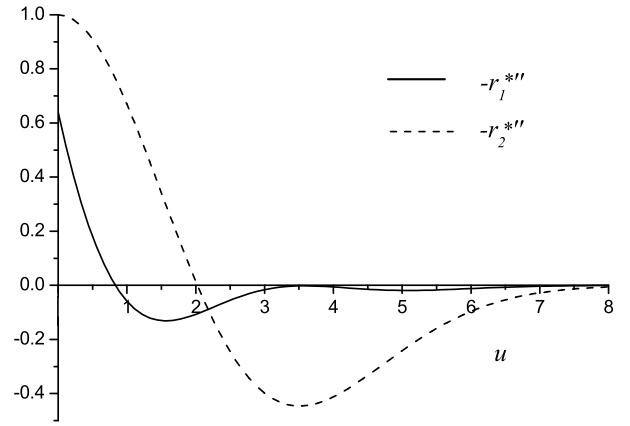


FIG. 4: Fixed point describing the interface in a medium with long-range correlated random bond disorder (LR RB FP) for $\hat{a} = 2$. The SR part $r_1(u)$ is a nonanalytic function with $r_1^{(0)}(0^+) \neq 0$. The LR part $r_2(u)$ is an analytic function. Here we report minus their second derivative.

eigenvalue $\lambda_1 = 1$ and reads

$$z_1(u) = \frac{1}{3} u r_1^{(0)}(u) + \frac{1}{2} r_1(u) + \frac{5}{6} r_2(u); \quad (63)$$

$$z_2(u) = \frac{1}{3} [u r_2^{(0)}(u) + r_2(u)]: \quad (64)$$

For other values of \hat{a} we solve Eq. (59) numerically using λ_1 as a shooting parameter and require an exponentially fast decay of $z_1(u)$ for large u . To compute the numerical solution, we need the initial conditions. Expanding Eq. (59) in a Taylor series, we obtain

$$z_1(0) = \frac{5[x^2(2^{\hat{a}+5}) + 5x(\hat{a}+5) + 3]}{3^{\hat{a}}(5-4-5)}; \quad (65)$$

$$z_1^{(0)}(0) = 0: \quad (66)$$

Apart from the marginal eigenvalue $\lambda_0 = 0$, the largest eigenvalue is λ_1 . It is shown for different $\hat{a} > 1.1$ in Table I. The negative sign of λ_1 reflects the stability of the LR RB FP. For $\hat{a} = 1.1$ we failed to compute the numerical solution with reasonable accuracy. However, the largest eigenvalue computed at LR RB FP λ_1 tends to 0 for $\hat{a} \rightarrow 1.1$ and the SR RB FP becomes unstable for $\hat{a} > 1.041$ with respect to LR-correlated disorder. Thus we expect that the LR RB FP is stable for $\hat{a} > 1.041$. Moreover, the largest eigenvalue within accessible accuracy is well approximated by $\lambda_1 = 0.1917(\frac{5}{3} - \frac{5}{3})$, which gives $\lambda_1 = 0.06$ for $\hat{a} = 1.1$.

Besides the roughness exponent, there is another universal quantity that is of interest. This is the displacement correlation function, which behaves like

$$\overline{u_q u_{-q}} = A_d q^{-(d+2)} : \quad (67)$$

Let us show that in contrast to systems with only SR-correlated disorder, this system, whose behavior is controlled by the LR RB FP, has a universal amplitude A_d . Indeed,

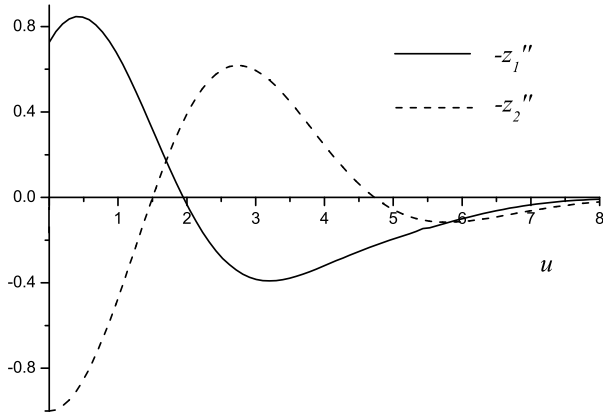


FIG. 5: Second derivative of eigenfunctions $z_1(u)$ and $z_2(u)$ computed at the LR RB FP for $\hat{\alpha} = 2$.

according to Eq. (51), the integral $\int_0^R du R_2^{\text{tr}}(u)$ is preserved along the flow and is fixed to its bare value Q , where we have introduced the actual renormalized correlator R_2^{tr} which is connected to R_2 given by Eq. (57) by the relation $R_1^{\text{tr}} = {}^4R_1(u=0)$ with 4R_1 given by

$$= \frac{Q^{1=5}}{(2)^{1=10}} \frac{\hat{\alpha}^{! 3=10}}{5(1+x)}; \quad (68)$$

where we used $\int_0^R du R_2^{\text{tr}}(u) = Q$. Then the amplitude can be written to one-loop order as follows [19]:

$$\begin{aligned} A_d &= \frac{1}{K_4} [R_1^{\text{tr}00}(0) - R_2^{\text{tr}00}(0)] \\ &= \frac{2}{K_4} (1+x) = Q^{2=5} B(\hat{\alpha}); \end{aligned} \quad (69)$$

where we have introduced the universal function

$$B(\hat{\alpha}) = \frac{8^{-2}}{(2)^{1=5}} (1+x(\hat{\alpha}))^{2=5} \frac{\hat{\alpha}^{! 3=5}}{5}; \quad (70)$$

Values for $x(\hat{\alpha})$ and for $B(\hat{\alpha})$ for different $\hat{\alpha}$ are shown in Table I.

VII. NONPERIODIC SYSTEMS: RANDOM FIELD DISORDER

We now address the problem of an elastic interface in a medium with LR-correlated RF disorder. We expect that similar to systems with uncorrelated disorder, this universality class also describes the depinning transition. To see that systems with RB disorder flow in the dynamics to the RF FP, one has to include either effects of a finite velocity or consider two-loop contributions, which go beyond of the scope of the present work; but we expect the mechanism to be the same as in Ref. [18].

Let us look for a solution of Eqs. (40) and (41), which decays exponentially fast at infinity as expected for RF disorder. From Eq. (41) it follows that (hereafter we drop the tilde on i)

$$\partial_u \begin{pmatrix} z_1 \\ z_2 \end{pmatrix} = \begin{pmatrix} 3 & 2 \\ 0 & 0 \end{pmatrix} \begin{pmatrix} z_1 \\ z_2 \end{pmatrix}; \quad (71)$$

Therefore, $R_1^{\text{tr}}(u)$ is preserved along the FRG flow fixing the roughness exponent to

$$\text{LR RF} = \frac{2}{3} + O(\epsilon^2; \epsilon^2; \epsilon^2); \quad (72)$$

which coincides with the Flory estimate. Introducing $y_1(u) = z_1(u)$, $y_2(u) = z_2(u)$ and fixing $y_1(0) = x$, $y_2(0) = 1$, we can rewrite the stationary form of Eqs. (40) and (41) as follows ($\hat{\alpha} = 3$):

$$(1 - 2y_1)y_1(u) + \frac{1}{2} \frac{d^2}{du^2} [y_1(u) + y_2(u)]^2 + [1 + x]y_1^{00}(u) = 0; \quad (73)$$

$$(\hat{\alpha} - 2y_2)y_2(u) + \frac{1}{2} \frac{d^2}{du^2} [y_1(u) + y_2(u)]^2 + [1 + x]y_2^{00}(u) = 0; \quad (74)$$

Equation (74) can be solved analytically giving

$$y_2(u) = \exp \left(-\frac{\hat{\alpha} u^2}{6(1+x)} \right); \quad (75)$$

Substituting the FP function (75) in Eq. (73), we obtain a closed differential equation for the function $y_1(u)$. Expanding around $u = 0$, we find

$$y_1^0(0) = \frac{1}{3} \frac{9x + 3\hat{\alpha} - 6x\hat{\alpha}}{6x\hat{\alpha}}; \quad (76)$$

$$y_1^{00}(0) = \frac{1}{3} \frac{\hat{\alpha} x}{9x + 1}; \quad (77)$$

$$y_2^0(0) = 0; \quad (78)$$

$$y_2^{00}(0) = \frac{\hat{\alpha}}{3(x+1)}; \quad (79)$$

Thus we can compute numerically the solution $y_1(u)$ for any fixed $\hat{\alpha}$ and $y_1(0) = x$, however only for special values of x does this solution decay exponentially at infinity. The corresponding solution can be computed using the shooting method as described above, using x as a shooting parameter (see Table II).

A pair of typical FP functions is shown in Fig. 6. Surprisingly, the function $y_1(u)$ obtained by shooting satisfies $\int_0^1 du y_1(u) = 0$, characteristic for RB-type correlations along the u direction. In other words, the LR RF FP is in fact of mixed type: RB for the SR part and RF for the LR part of the disorder correlator. This can be understood as follows: Consider the flow of $R_1^{\text{tr}}(u)$. It is obtained by integrating the l.h.s. of Eq. (73) from 0 to infinity, and by inserting

TABLE II: Long-range correlated random field disorder. Shooting parameter $x = y_1(0)$, the maximal eigenvalue and the universal amplitude for different values of $\hat{\alpha}$.

$\hat{\alpha}$	$x(\hat{\alpha})$	λ_1	$B(\hat{\alpha})$
1.1	0.562872	0.1	140.43
1.2	0.525082	0.2	142.23
1.3	0.496948	0.3	144.27
1.4	0.475110	0.4	146.44
1.5 ^a	0.457638	0.5	148.66
2.0 ^b	0.404989	1.0	159.66
3.0 ^c	0.362329	2.0	179.04

^aRandom lines in planar interface ($d = 2, a = 1$).

^bRandom lines in a 3d manifold ($d = 3, a = 2$).

^cRandom planes in a 3d manifold ($d = 3, a = 1$).

$$\lambda_1 = \hat{\alpha} = 3:$$

$$\partial_u \int_0^{\lambda_1} du y_1(u) = \lambda_1 \int_0^{\lambda_1} du y_1(u) + \frac{1}{2} \frac{d}{du} [y_1(u) + y_2(u)]^2 \Big|_{u=0} (1+x) y_1^0(0); \quad (80)$$

where we have used the fact that most terms in the FRG-equation (73) are total derivatives. Finally, we remark that the second line of Eq. (80) cancels exactly provided that $y_2(u)$ is an analytical function, leaving us with

$$\partial_u \int_0^{\lambda_1} du y_1(u) = \lambda_1 \int_0^{\lambda_1} du y_1(u): \quad (81)$$

This means that for LR-correlated disorder, i.e., $\hat{\alpha} > 1$, the integral of y_1 indeed scales to 0. A nontrivial fixed point is possible at two-loop order for depinning. We remind the reader that in [18] it was shown that at two-loop order and for SR-correlated disorder, new terms arise in the FRG equation, which do *not* integrate to 0. Indeed, this is the mechanism that leads to a breakdown of the result $\lambda_{SRFP} = \hat{\alpha} = 3$ at depinning. The same terms will appear here. We expect that the additional diagrams due to LR correlations do not exactly cancel these terms, especially since these terms are proportional to the derivative at the cusp, and LR disorder will probably remain analytic, thus not contribute to the anomalous terms. These considerations let us expect that at two-loop order the integral of $y_1(u)$ will be small, but nonzero.

Let us finally check the stability of the SR RF FP and new LR RF FP. At the SR RF FP, the roughness is given by $\lambda_{SRFP} = \hat{\alpha} = 3$, and thus we expect the crossover from the SR universality to LR at $\hat{\alpha} > 3$, which follows from the condition $\lambda_{SRFP} = \lambda_{LRRF}$. To check the stability of the FPs, we follow the strategy used for the RB case and linearize the flow

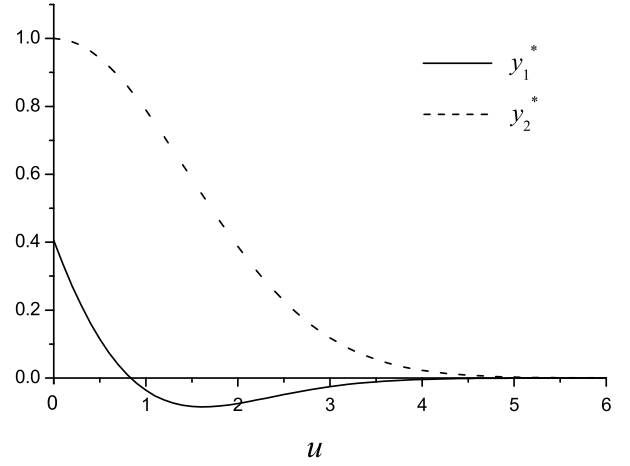


FIG. 6: Fixed point describing the interface in a medium with long-range correlated random field disorder (LR RF FP) for $\hat{\alpha} = 2$. The SR correlator $y_1(u)$ has a cusp at origin and formally corresponds to RB type of correlation in direction u . The LR correlator $y_2(u)$ is an analytic function of RF type.

equations about the RF FPs. We obtain

$$\begin{aligned} (1 - \lambda_1) z_1(u) + \lambda_1 u z_1^0(u) &= \frac{d^2}{du^2} [y_1(u) + y_2(u)] \\ &= [y_1(u) + y_2(u)] + (1+x) z_1^0(u) \\ &+ A_0 y_1^0(u) = z_1(u); \end{aligned} \quad (82)$$

$$\begin{aligned} (\hat{\alpha} - \lambda_1) z_2(u) + \lambda_1 u z_2^0(u) &+ (1+x) z_2^0(u) \\ &+ A_0 y_2^0(u) = z_2(u); \end{aligned} \quad (83)$$

where we have introduced $A_0 = z_1(0) + z_2(0)$. First, we prove our conclusion on the stability of SR RF FP with respect to LR-correlated disorder. To that end, we solve Eq. (60) assuming that $\lambda_1 = \lambda_1^{SR} = 3$ and $x = y_1^{SR}(0) = 2.9$. We obtain that $z_2 = \exp[\lambda_1^{SR} u^2 / (2 y_1^{SR})]$ and the corresponding eigenvalue $\lambda_{max} = \hat{\alpha}^3 \lambda_1^{SR}$. Therefore, indeed the SR RF FP becomes unstable with respect to LR disorder for $\hat{\alpha} > 3$.

We now focus on the stability of the LR RF FP. Analysis of the linearized flow equations (82) and (83) shows that there is at least one eigenvector $z_1^{(0)} = u^{-1} y_1(u) - 2 y_1$ with marginal eigenvalue $\lambda_0 = 0$, which corresponds to the freedom of rescaling. For arbitrary λ , Eq. (83) can be solved analytically,

$$z_2(u) = \frac{A_0 - u^2}{3(2 + 3x)(1+x)^2} \exp\left[-\frac{\hat{\alpha} u^2}{6(1+x)}\right]; \quad (84)$$

We are free to fix the length of the eigenvectors, for instance by the condition $z_2(0) = 1$, which gives

$$A_0 = \frac{1}{\hat{\alpha}} (2\hat{\alpha} + 3)(1+x); \quad (85)$$

Thus to find the eigenvalue λ and the eigenfunction z_1 , we have to solve Eq. (82) with condition $z_1(0) = A_0 - 1$ and

require an exponentially fast decay for large u . We need the initial conditions that can be found by expanding Eq. (82) in a Taylor series,

$$z_1(0) = 1 - \frac{1}{\Lambda} (2\Lambda + 3)(1+x); \quad (86)$$

$$z_1^0(0) = \frac{1}{\Lambda} [9 - 2 + (12\Lambda - 9)(x+1) + \Lambda^2(4x+7)] \\ \frac{1}{\Lambda} (6x+9) = 2\Lambda - 9x - 6x\Lambda + 3\Lambda^2; \quad (87)$$

$\Lambda = 2$ is the only case in which we succeeded to find a completely analytical solution (see Fig. 7). It has $\Lambda_1 = 1$ and reads

$$z_1(u) = u y_1^0(u) - \frac{1}{2} y_1(u) - \frac{3}{2} y_2(u); \quad (88)$$

$$z_2(u) = u y_2^0(u) + y_2(u); \quad (89)$$

For other values of Λ , Eq. (89) remains correct, while to obtain $z_1(u)$, we solve Eq. (82) numerically, using Λ as a shooting parameter. As can be seen from Table II, the largest eigenvalue satisfies $\Lambda_1(\Lambda) = 1 - \frac{3}{\Lambda} (\Lambda_1^{SR} - \Lambda_1^{LR})$. This result can be obtained analytically as follows. Integrating Eq. (82) from 0 to 1, we get the condition

$$\int_0^1 du z_1(u) - \frac{1}{\Lambda} = 0; \quad (90)$$

proving that as long as $z_1(u) \notin 0$, one has $\Lambda = 1 - \frac{3}{\Lambda}$. Therefore, the LR RF FP is stable for $\Lambda > 1$. Inserting this value of Λ back into Eq. (82), we obtain after some simplifications

$$0 = \frac{1}{3} \frac{d}{du} [u z_1(u)] - \frac{d^2}{du^2} [Y(u) z_1(u) + W(u)]; \\ Y(u) = y_1(u) - y_1(0) + y_2(u) - y_2(0); \quad (91) \\ W(u) = z_2(u) [y_1(u) + y_2(u)] - y_1(0) [z_1(0) + z_2(0)];$$

The first equation can be integrated with the result

$$\frac{1}{3} u z_1(u) = \frac{d}{du} [Y(u) z_1(u) + W(u)]; \quad (92)$$

This is equivalent to

$$z_1 - Y^0 - \frac{1}{3} u + z_1^0 Y = -W^0; \quad (93)$$

The homogenous equation reads

$$[u z_1 Y]^0 = \frac{1}{3} \frac{u}{Y}; \quad (94)$$

Its solution is

$$z_1(u) = \frac{C}{Y(u)} \exp \left[-\frac{1}{3} \int_0^u ds \frac{s}{Y(s)} \right]; \quad (95)$$

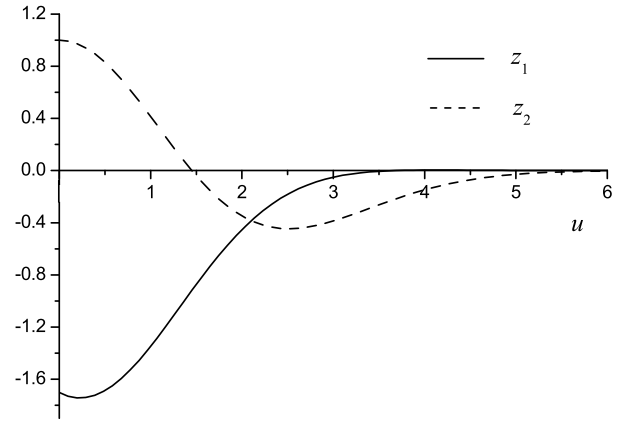


FIG. 7: Eigenfunctions $z_1(u)$ and $z_2(u)$ computed at the LR RF FP for $\Lambda = 2$.

with some constant C . A solution to the inhomogeneous equation is obtained by replacing C by $C(u)$, and inserting the latter into Eq. (93). This yields

$$C(u) = \frac{1}{Y(u)} \int_0^u dt W^0(t) \exp \left[-\frac{1}{3} \int_t^u ds \frac{s}{Y(s)} \right]; \quad (96)$$

Putting together everything, we obtain

$$z_1(u) = \frac{1}{Y(u)} \int_0^u dt W^0(t) \exp \left[-\frac{1}{3} \int_t^u ds \frac{s}{Y(s)} \right]; \quad (97)$$

Let us now compute the universal amplitude defined by Eq. (67). According to Eq. (71), the integral $\int_0^1 du z_2(u)$ is preserved along the FRG flow and can be fixed by its bare value Q . The relation between the actual renormalized disorder Λ_2^{tr} and the rescaled disorder $\Lambda_2(u)$ given by Eq. (75) reads $\Lambda_2^{tr} = \Lambda_2(u=1)$. We obtain

$$= \frac{Q^{1=3}}{\Lambda_2^{1=3}} \frac{2\Lambda}{3(1+x)} \Big|_{\Lambda=2}; \quad (98)$$

where we have fixed $\int_0^1 du z_2(u) = Q$. Then the amplitude can be written as

$$A_d = \frac{1}{K_4} [\Lambda_1^{tr}(0) + \Lambda_2^{tr}(0)] \\ = \frac{1}{K_4} (1+x) = \Lambda_2^{1=3} Q^{2=3} B(\Lambda); \quad (99)$$

with the universal functions given by

$$B(\Lambda) = 8^{-2} (1+x)^{2=3} \frac{2\Lambda}{3} \Big|_{\Lambda=2}; \quad (100)$$

Values of $B(\Lambda)$ for different Λ are shown in Table II.

Depinning. We are now in the position to study the depinning transition, which we expect is controlled by the LR RF

TABLE III: Periodic systems with LR correlated disorder. The shooting parameter: $y_1(0)$ and two first eigenvalues for different ϵ .

ϵ	$y_1(0)$	1	2
0	0.00971	0.0	
1=3	0.01089	0.333	4.089
1=2	0.01183	0.500	0.500
2=3 ^a	0.01348	0.667	0.280
0.8	0.01645	0.800	0.125
0.9	0.02346	0.900	0.013

^aCorresponds to $d = 2$, $a = 1$, i.e., line defects (e.g., dislocations) along the plane of a CDW.

FP. The dynamic critical exponent z defined by Eq. (45) is given to one-loop order by

$$z = 2 - \frac{\epsilon}{3} + \frac{\epsilon^2}{9} + O(\epsilon^3; \epsilon^2; \epsilon); \quad (101)$$

where we have used Eqs. (77) and (79), which give $y_1^0(0) + y_2^0(0) = 1=3$ $\epsilon=9$. Other exponents can be computed using scaling relations (47) and (46), for example

$$z = 1 - \frac{\epsilon}{6} + \frac{\epsilon^2}{18} + O(\epsilon^3; \epsilon^2; \epsilon); \quad (102)$$

It is remarkable that for $\epsilon > 3$, the exponent z is larger than 1, and z is larger than 2. This seems to imply some different physics - yet to be understood - in the avalanche process, which makes the motion slower near depinning than in the SR case. The analyticity of z seems to suggest some smoother motion at large scale, while short-scale motion remains jerky and avalanche-like. Finally, note that at the SR RF FP, $z_{SR} = 2 - 2\epsilon=9$, $z_{SR} = 1 - \epsilon=9$, and thus, the exponents are continuous functions of ϵ and ϵ .

VIII. PERIODIC SYSTEMS

We now study periodic systems with disorder correlator given by Eq. (4), which we can refer to as an XY model with LR-correlated defects. The results for CDWs with LR-correlated disorder defined by correlator (15) can then be obtained by substituting $\epsilon = 1 = 4 - d$. It is sufficient to consider the system with the period fixed to 1, since other systems can be related to the latter using the freedom to rescale. As a consequence, the roughness exponent for periodic systems is $\alpha = 0$. At variance with interfaces, we introduce reduced parameters according to $y_1(u) = \bar{y}_1(u)$, $A = y_1(0) + y_2(0)$, and $\epsilon = \epsilon$. Then the fixed-point equations can be written as follows:

$$\epsilon y_1(u) - \frac{1}{2} \frac{d^2}{du^2} [\bar{y}_1(u) + y_2(u)]^2 + A y_1^0(u) = 0; \quad (103)$$

$$y_2(u) + A y_2^0(u) = 0; \quad (104)$$

Equation (104) can be solved analytically. Its solution is

$$y_2 = y_2(0) \cos(2\pi u); \quad A = 1=(2\pi)^2; \quad (105)$$

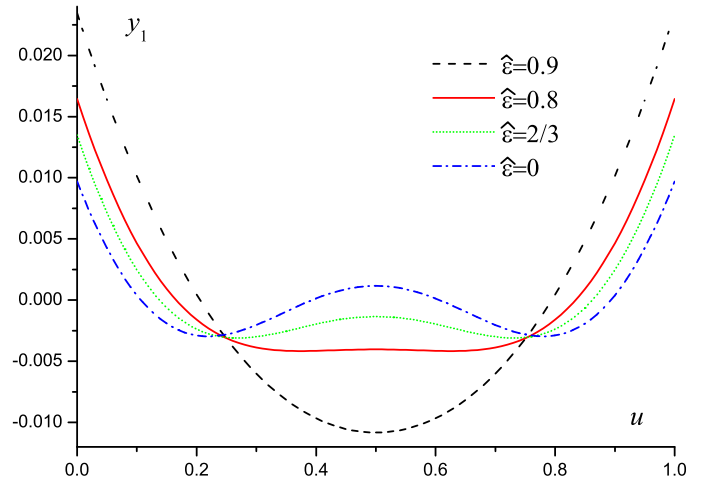


FIG. 8: (Color online) Fixed point of a periodic system with LR correlated disorder. The SR disorder correlator $y_1(u)$ computed for different values of ϵ .

Equation (103) can be solved analytically for $\epsilon = 0$,

$$y_1 = y_1(0) + y_2(0) [1 - \cos(2\pi u)] \frac{1}{2} \frac{P}{2y_2(0) [1 - \cos(2\pi u)]}; \quad (106)$$

The coefficients $y_1(0)$ are determined by potentiality of the y_1 , i.e., from the conditions

$$\frac{d}{du} y_1(u) = \frac{d}{du} y_2(u) = 0; \quad (107)$$

and the identity $y_1(0) + y_2(0) = 1=(2\pi)^2$. They read

$$y_1(0) = 1=(2\pi)^2 \quad 1=64; \quad (108)$$

$$y_2(0) = 1=64; \quad (109)$$

For $\epsilon > 0$, Eq. (103) can be written in the following form:

$$\epsilon y_1(u) - \frac{1}{2} \frac{d^2}{du^2} [\bar{y}_1(u) + y_2(u)]^2 - \frac{y_1(u)}{2} = 0; \quad (110)$$

where $y_2(u)$ is given by Eq. (105) with $y_2(0) = 1=(2\pi)^2 y_1(0)$. Expanding Eq. (110) in a Taylor series about $u = 0$, we find that $y_1^0(0) = \frac{1}{1=(2\pi)^2} \frac{y_1(0)}{(1 - \epsilon)}$. Thus for any fixed $0 < \epsilon < 1$ and $y_1(0)$ we have only one solution $y_1(u)$, but only for a specific $y_1(0)$ this solution fulfills the condition $y_1(1) = y_1(0)$. To find this value, we employ the shooting method using $y_1(0)$ as a shooting parameter. The values of $y_1(0)$ computed for different ϵ are summarized in Table III. The corresponding eigenfunctions $y_1(u)$ are depicted in Fig. 8.

While the roughness exponent is zero, the system forms a Bragg glass phase with a slow growth of the displacements according to

$$\overline{(u_x - u_y)^2} = A_d \ln |x|; \quad (111)$$

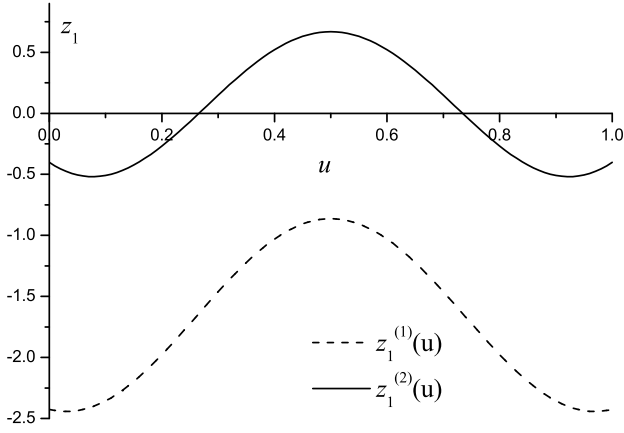


FIG. 9: Two first eigenvectors computed at the LR periodic FP. Eigenfunctions $z_1^{(1)}(u)$ and $z_1^{(2)}(u)$ for $n = 2=3$.

where A_d is a universal amplitude, which to one-loop order is given by

$$A_d^{(LR)} = \frac{2K_d}{K_4} [z_1(0) + z_2(0)] = \frac{1}{2}; \quad (112)$$

where we have restored the factor of $1=K_4$ previously absorbed in z_i . The SR periodic FP is characterized by $A_d^{(SR)} = n=18 + O(n^2)$. It is interesting to compare Eq. (112) with the prediction of the Gaussian variational approximation for the SR disorder case $A_{d;GVA}^{(SR)} = n=(2^2)$. We expect the crossover between LR and SR FPs at $A_d^{(LR)} = A_d^{(SR)}$, i.e., LR disorder to be relevant for

$$n < \frac{9}{2} \quad 0.912; \quad (113)$$

We now check the stability of the SR and LR periodic FPs. The flow equations linearized about the FP read

$$n z_1(u) = \frac{d^2}{du^2} [y_1(u) + y_2(u)] [z_1(u) + z_2(u)] + A z_1^{(0)}(u) + A_0 y_1^{(0)}(u) = z_1(u); \quad (114)$$

$$z_2(u) + A z_2^{(0)}(u) + A_0 y_2^{(0)}(u) = z_2(u); \quad (115)$$

where we have introduced $A_0 = z_1(0) + z_2(0)$. Let us recall that the SR FP is unstable with respect to nonpotential perturbations even in the subspace of SR disorder. Indeed, the SR periodic FP,

$$z_1(u) = \frac{n}{6} \frac{1}{6} u(1-u); \quad z_2(u) = 0; \quad (116)$$

has in the SR subspace the positive eigenvalue $\lambda_1 = 1$, corresponding to the nonpotential eigenfunction $z_1 = 1$. All other eigenfunctions are potential, i.e., fulfill condition (107), and have negative eigenvalues [45]. If we add LR-correlated disorder, the solution of Eq. (115) yields

$$z_2(u) = \cos 2u; \quad (117)$$

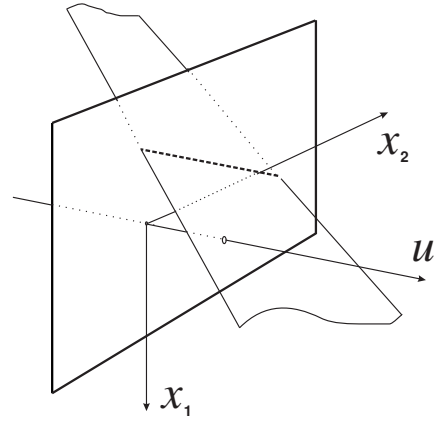


FIG. 10: 2d domain wall moving in 3D magnet with fully isotropic planar defects.

The corresponding eigenvalue $\lambda_{SR} = 1 - n^2=9$ confirms our estimation for the stability of the SR periodic FP (113). For the LR periodic FP, we still have Eq. (117) with

$$A_0 = \frac{1}{1 - 4^2 y_1(0)}; \quad z_1(0) = A_0 - 1; \quad (118)$$

Equation (114) has a periodic solution only for a discrete set of eigenvalues λ_i (the first two are shown in Table III). It follows from the table that $\lambda_1 = n > 0$. In analogy with the SR periodic FP, the LR periodic FP is unstable with respect to a nonpotential perturbation corresponding to λ_1 . The latter is obtained by integrating Eq. (115) over one period,

$$\left(\frac{n}{2} \right) \int_0^1 du z_1(u) = 0; \quad (119)$$

As long as the integral does not vanish, this gives the reported eigenvalue $\lambda_1 = n$. Indeed, as can be seen from Fig. 9, we have $\int_0^1 du z_1^{(1)}(u) \neq 0$ and $\int_0^1 du z_1^{(n)}(u) \neq 0$ for $n \geq 2$.

Depinning. We now focus on the depinning transition of the periodic system with LR-correlated disorder. At the LR periodic FP, we have

$$y_1^{(0)}(0) = 1 + \frac{n}{3} 4^2 y_1(0); \quad (120)$$

$$y_2^{(0)}(0) = 4^2 y_2(0); \quad (121)$$

and thus $y_1^{(0)}(0) + y_2^{(0)}(0) = n=3$. The dynamic critical exponent z defined by Eq. (45) reads to one-loop order

$$z^{LR} = 2 - \frac{n}{3} + O(n^2; n^2; n); \quad (122)$$

Therefore, for periodic systems $z^{LR} = z^{SR}$ to one-loop order.

IX. FULLY ISOTROPIC EXTENDED DEFECTS

In this section, we briefly examine the effect of a defect distribution isotropic in the whole $(x;u)$ space. Consider first

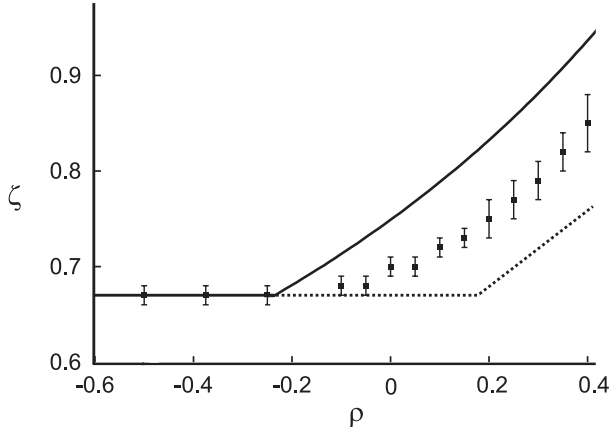


FIG. 11: The roughness exponent of the optimal paths on the plane with isotropically correlated disorder (data taken from Ref. [48]). Solid line $\zeta = 3/(4 - 2) = 3/2$ is the roughness exponent of the elastic string on the plane with fully isotropic long-range correlated disorder. Dashed line $\zeta = (3 + 2)/5 = 5/5$ is the roughness exponent of the elastic string on the plane with disorder correlated only along the string.

interfaces in random bond type disorder. From Eqs. (5) and (9), one finds

$$R(\mathbf{x}; u) = \frac{V_{RB}(\mathbf{x}; u)V_{RB}(0; 0)}{V_{LR}^2} \frac{1}{k^2 + u^2} \quad (123)$$

and thus the u and x dependences are coupled in the bare correlator. For the present discussion, we consider N , the number of components of u , arbitrary, hence $D = N + d$. We recall that $a = D - d$. The question of to which universality class this model belongs is subtle. It turns out that it does not correspond to LR disorder in internal space, but rather SR disorder in internal space and LR disorder in the u direction, hence $R_2 = 0$ but $R_1(u)$ long-range in u . To see this, let us consider at fixed u the integral $\int d^d x R(\mathbf{x}; u)$. We can distinguish two cases, as follows.

(i) For $a > d$, this integral is convergent at large x , hence we clearly have SR disorder in the x direction, and $R_1(u) \sim u^{-(a-d)}$ at large u . This, however, is LR disorder in u . This case has been studied using FRG and yields, for $a < a_c(d; N)$, a roughness exponent given by the Flory value $(a; d) = (4 - d)/(4 + a - d)$. The value $a_c(d; N)$ can be estimated using the value for the SR disorder roughness exponent, by requiring $(a_c(d; N); d) = \zeta_{SRB}(d; N)$ (small deviations can arise as discussed in [7]).

(ii) For $a < d$, the situation is more subtle and one may be tempted to argue, since $\int d^d x R(\mathbf{x}; u)$ diverges in the infrared, that disorder LR in x is produced. This is, however, not the case, as can be seen on the Fourier transform $R(q; P)$, where P is the momentum associated with u , and q with x . One has $R(q; P) \sim (q^2 + P^2)^{(a-d-N)/2}$, which has a well defined limit $R(q = 0; P) = P^{a-d-N}$. This corresponds again, as we argue, to a SR correlator in space with $R_1(u) \sim R_1(0) \sim u^{-(a-d)}$. As is often the case, LR models require some trivial subtractions. The subtracted correlator

$R(\mathbf{x}; u) - R(\mathbf{x}; 0)$ has indeed a convergent integral $\int d^d x$ at large u , while subtracting a u -independent piece does not change the model. The critical case $a = d$ is described by the logarithmic model $R(\mathbf{x}; u) - R(\mathbf{x}; 0) \sim \ln |\mathbf{x}|$ which has $\zeta = (4 - d)/4$ in all dimensions [7].

To summarize, isotropic distributions of defects isotropic in the $(\mathbf{x}; u)$ space also yield LR models, but not of the type (4) studied here. For isotropic line defects, one finds $\zeta = (4 - d)/(3 + N)$ (i.e., $\zeta = 3/4$ for a directed polymer in $D = 1 + 1$, $\zeta = 3/5$ in $D = 1 + 2$, and for an interface $D = 2 + 1$, $\zeta = 2/5$). Isotropic planar defects yield $\zeta = (4 - d)/(2 + N)$, hence $\zeta = 2/3$ for a $(D = 2 + 1)$ -dimensional interface. This case is illustrated in Fig. 10. Note that in that case there are infinitely many lines of defects inside the interface with random directions (the intersections of the planar defects with the interface gives lines), but that this does not suffice to create power-law correlations in internal space, as can be seen from the example in which the planar defects are orthogonal to the interface.

In Ref. [48], the universal properties of the optimal paths on the plane with isotropically correlated random potential which correlation decays as r^{2-d} were studied using numerical simulations. This model is believed to belong to the same universality class as the one-dimensional ($d = 1$) elastic interface in a medium with fully isotropic long-range correlated disorder with $a = 1 - d$. The roughness exponent of the shortest paths computed in Ref. [48] for different values of d is shown in Fig. 11. In the optimal path model, the elasticity is generated by disorder and the long-range correlated disorder can generate the long-range elasticity, which would decrease the path roughness and account for the deviation from our prediction. The effective elasticity is expected to be described in terms of the exponent ν , which computation requires the two-loop consideration.

Finally in the periodic case, such as for CDWs, isotropic disorder in the full space $(\mathbf{x}_k; \mathbf{x}_2)$ again leads to correlations (15), but now the function $g(\mathbf{x}_k - \mathbf{x}_k')$ decays exponentially beyond a length scale set by the disorder period (as can be seen in Fourier space considering the discrete P modes). Hence the problem is described by the standard (SR) random periodic class.

X. CONCLUSION

We have studied elastic interfaces and periodic systems in a medium with LR correlated disorder, both in equilibrium and at the depinning transition. This type of long-range correlation exists in the internal space of the manifold, and we have discussed how it can be realized in terms of extended defects, or anisotropic defects with a broad distribution of lengths. Using a dynamic formalism, we derived the FRG flow equations for the SR and LR parts of the disorder correlator and found three new FPs, which describe three new universality classes. All new FPs are characterized by a nonanalytic SR part of the disorder correlator and an analytic LR part. We have computed the corresponding exponents and universal amplitudes in a double expansion in $\epsilon = 4 - d$ and $\epsilon = 4 - a$. For RB

type of disorder, we find that the LR correlation of disorder is relevant for $\nu > 1.041$ and results in the roughness exponent $\alpha = 5$, while for $\nu < 1.041$ the scaling behavior is controlled by the SR RB FP with $\alpha = 0.208298$. We find that the presence of RF disorder results in a mixed FP with the SR correlator corresponding formally to RB type of disorder and an analytic RF LR correlator. The LR RF FP, which is also expected to control the depinning transition, is stable for $\nu > 1$ giving $\alpha = 3$ and $\beta = 1$ $\nu = 6 + \alpha = 18$. The LR correlated periodic FP is stable for $\nu < 0.912$ and gives a slow logarithmic growth of displacements with universal amplitude $A_{dR} = 2 = (2^2)$. It is remarkable that this type of disorder yields an exponent for the velocity-force characteristics that can be larger than unity and a dynamical exponent larger than 2. This striking behavior might be relevant for experiments, and gives a strong motivation for numerical studies of the problem, e.g., to understand the nature of motion at the

depinning transition in these systems.

Acknowledgments

We thank Dima Feldman and Heiko Rieger for useful discussions, and the Kavli Institute for Theoretical Physics at the University of California, Santa Barbara for hospitality while this work was being finished. This research was supported in part by the National Science Foundation under Grant No. PHY99-07949. A.A.F. acknowledges support from the European Commission under Contract No. MIF1-CT-2005-021897. P.L.D. and K.J.W. are supported by Agence Nationale de la Recherche under Contract No. 05-BLAN-0099-01.

-
- [1] D. S. Fisher, Phys. Rep. **301**, 113 (1998).
 - [2] M. Kardar, Phys. Rep. **301**, 85 (1998).
 - [3] S. Brazovskii and T. Nattermann, Adv. Phys. **53**, 177 (2004).
 - [4] S. Lemerle, J. Ferre, C. Chappert, V. Mathet, T. Giamarchi, and P. Le Doussal, Phys. Rev. Lett. **80**, 849 (1998).
 - [5] D. Wilkinson and J.F. Willemsen, J. Phys. A **16**, 3365 (1983).
 - [6] G. Grüner, Rev. Mod. Phys. **60**, 1129 (1988).
 - [7] G. Blatter, M.V. Feigel'man, V.B. Geshkenbein, A.I. Larkin, and V.M. Vinokur, Rev. Mod. Phys. **66**, 1125 (1994).
 - [8] T. Nattermann and S. Scheidl, Adv. Phys. **49**, 607 (2000).
 - [9] T. Giamarchi and P. Le Doussal, Phys. Rev. Lett. **72**, 1530 (1994); Phys. Rev. B **52**, 1242 (1995).
 - [10] M. Mezard and G. Parisi, J. Phys. A **23**, L1229 (1990).
 - [11] S.E. Korshunov, Phys. Rev. B **48**, 3969 (1993).
 - [12] D. S. Fisher, Phys. Rev. Lett. **56**, 1964 (1986).
 - [13] A.I. Larkin, Sov. Phys. JETP **31**, 784 (1970).
 - [14] T. Nattermann, S. Stepanow, L.-H. Tang, and H. Leschhorn, J. Phys. II France **2**, 1483 (1992).
 - [15] H. Leschhorn, T. Nattermann, S. Stepanow, and L.-H. Tang, Ann. Phys. (Leipzig) **6**, 1 (1997).
 - [16] O. Narayan and D. S. Fisher, Phys. Rev. B **48**, 7030 (1993).
 - [17] P. Chauve, P. Le Doussal, and K.J. Wiese, Phys. Rev. Lett. **86**, 1785 (2001).
 - [18] P. Le Doussal, K.J. Wiese, and P. Chauve, Phys. Rev. B **66**, 174201 (2002).
 - [19] P. Le Doussal, K.J. Wiese, and P. Chauve, Phys. Rev. E **69**, 026112 (2004).
 - [20] P. Le Doussal and K.J. Wiese, Phys. Rev. B **68**, 174202 (2003).
 - [21] L. Roters and K.D. Usadel, Phys. Rev. E **65**, 027101 (2002).
 - [22] L. Roters, S. Lübeck, and K. D. Usadel, Phys. Rev. E **66**, 026127 (2002).
 - [23] A. Rosso, A.K. Hartmann, and W. Krauth, Phys. Rev. E **67**, 021602 (2003).
 - [24] A.A. Middleton, P. Le Doussal, and K.J. Wiese, e-print cond-mat/0606160; P. Le Doussal, e-print cond-mat/0605490; A. Rosso, P. Le Doussal, and K.J. Wiese, e-print cond-mat/0610821.
 - [25] P. Chauve, T. Giamarchi, and P. Le Doussal, Phys. Rev. B **62**, 6241 (2000).
 - [26] S.N. Dorogovtsev, Phys. Lett. **76A**, 169 (1980).
 - [27] D. Boyanovsky and J.L. Cardy, Phys. Rev. B **26**, 154 (1982).
 - [28] I.D. Lawrie and V.V. Prudnikov, J. Phys. C **17**, 1655 (1984).
 - [29] A.A. Fedorenko, Phys. Rev. B **69**, 134301 (2004).
 - [30] A. Weinrib and B.I. Halperin, Phys. Rev. B **27**, 413 (1983).
 - [31] E. Korutcheva and F. Javier de la Rubia, Phys. Rev. B **58**, 5153 (1998).
 - [32] V.V. Prudnikov and A.A. Fedorenko, J. Phys. A **32**, L399 (1999); V.V. Prudnikov, P.V. Prudnikov, and A.A. Fedorenko, Phys. Rev. B **62**, 8777 (2000).
 - [33] L. Civalé, A.D. Marwick, T.K. Worthington, M.A. Kirk, J.R. Thompson, L. Krusin-Elbaum, Y. Sun, J.R. Clem, and F. Holtzberg, Phys. Rev. Lett. **67**, 648 (1991).
 - [34] D.R. Nelson and V.M. Vinokur, Phys. Rev. Lett. **68**, 2398 (1992).
 - [35] T. Emig and T. Nattermann, e-print cond-mat/0604345.
 - [36] T. Hwa, P. Le Doussal, D.R. Nelson, and V.M. Vinokur, Phys. Rev. Lett. **71**, 3545 (1993).
 - [37] L. Civalé, L. Krusin-Elbaum, J.R. Thompson, R. Wheeler, A.D. Marwick, M.A. Kirk, Y.R. Sun, F. Holtzberg, and C. Feild, Phys. Rev. B **50**, 4102 (1994).
 - [38] T. Hwa, D.R. Nelson, and V.M. Vinokur, Phys. Rev. B **48**, 1167 (1993).
 - [39] P. Chauve, Ph.D. thesis, Université de Paris XI Orsay, 2000; <http://www.lpt.ens.fr/~chauve/>
 - [40] P. Chauve, P. Le Doussal, and T. Giamarchi, Phys. Rev. B **61**, R11906(2000).
 - [41] Y. Yamazaki, A. Holz, M. Ochiai, and Y. Fukuda, Physica A **150**, 576 (1988).
 - [42] C. Vazquez, R. Paredes, A. Hasmy, and R. Jullien, Phys. Rev. Lett. **90**, 170602 (2003).
 - [43] D.E. Feldman and R.A. Pelcovits, Phys. Rev. E **70**, 040702(R) (2004).
 - [44] E. Medina, T. Hwa, M. Kardar, and Y.-C. Zhang, Phys. Rev. A **39**, 3053 (1989).
 - [45] P. Le Doussal and K.J. Wiese, Phys. Rev. E **68**, 046118 (2003).
 - [46] P. Le Doussal and K.J. Wiese, Phys. Rev. E **67**, 016121 (2003).
 - [47] P. Le Doussal, Phys. Rev. Lett. **96**, 235702 (2006) and to be published.
 - [48] R. Schorr and H. Rieger, Eur. Phys. J. B, **33**, 347 (2003).